Comparison of Dielectric and Viscoelastic Relaxation Spectra of Polyisoprene

Keiichiro Adachi,* Hirotsugu Yoshida, Fumiaki Fukui, and Tadao Kotaka

Department of Macromolecular Science, Faculty of Science, Osaka University, Toyonaka, Osaka 560, Japan

Received November 6, 1989; Revised Manuscript Received January 4, 1990

ABSTRACT: Measurements of complex dielectric constant ϵ^*, shear viscosity η_0, and complex shear modulus G^* were carried out on narrow molecular weight distribution *cis*-polyisoprenes (*cis*-PI) to determine their dielectric relaxation, $g(\tau)$, and viscoelastic relaxation, $H(\tau)$, spectra. For each sample the spectra were compared over a wide range of time scale covering the wedge-type to the box-type region of the viscoelastic spectrum. The viscoelastic relaxation time, τ_V, agreed with the dielectric normal-mode relaxation time, τ_n, while the relaxation time at the maximum of the wedge-type spectrum agreed with the dielectric segmental-mode relaxation time, τ_s. In the wedge-type region, the slope of the log $H(\tau)$ vs log τ plot changed at the time scale of the transition from the Rouse-like motions to the segmental motions as τ decreased. For unentangled *cis*-PIs with a molecular weight, M_w, less than the characteristic molecular weight, M_c, the observed τ_n agreed with the longest Rouse relaxation time calculated with η_0. For entangled *cis*-PIs with $M_w > M_c$, the shape of the spectra $H(\tau)$ and $g(\tau)$ differed in the terminal region.

Introduction

Although a number of studies have been made on viscoelastic and dielectric properties of linear polymers,[1-4] close comparison between them has not yet been made extensively.[3,5-7] Especially comparison of the behavior in the so-called terminal-to-flow region has never been reported presumably because the dielectric response is usually inactive for the molecular motions in this long time-scale region. However, Stockmayer suggested a long time ago that what he called a type A polymer having the dipole moment aligned in the same direction parallel along the chain contour may exhibit dielectric relaxation due to fluctuation of the end-to-end vector of the molecules.[4] Thus the relaxation mode that we called dielectric *normal-mode* relaxations[8,9] should reflect polymer chain dynamics in this long time-scale region. Several years ago we realized that *cis*-polyisoprene (*cis*-PI) belongs to the type A polymer and extensively studied the dielectric normal-mode process of this polymer.[8-11]

As is well-known, the fluctuation of the end-to-end vector of a type A polymer is an essential factor governing the terminal modes of the viscoelastic as well as dielectric normal-mode relaxations, regardless of the polymer chains being in the unentangled state[12,13] or in the entangled state.[14-16] We thus expect that close comparison between them should provide us with meaningful information to understand the dynamics of polymers in general from a molecular point of view.

Interestingly *cis*-PI also exhibits a dielectric segmental-mode process that appears in the frequency range much higher than the normal-mode process.[8-11] This segmental-mode relaxation is closely related to the glass transition of the polymer[1,3] and was called the primary α_a process.[3] The dielectric segmental-mode relaxation in general corresponds to the so-called wedge-type portion of viscoelastic relaxation spectra of linear flexible-chain polymers.[1] It is thus easily conceivable that the wedge-type spectrum is related to the local segmental motions and the higher order modes of Rouse-like[12] motions. However, again the correlation between the dielectric and viscoelastic relaxation spectra in this region has not been well understood. Recently, Ngai, Mashimo, and Fytas[6,7] compared the behavior of the segmental motions detected with various probes including dielectric spectroscopy.

In this paper we first compare viscoelastic and dielectric relaxation spectra of the same *cis*-PI samples over a wide range of time domain covering the so-called wedge-type to box-type regions.[1] By doing so we expect to clarify the overall relationship between the dielectric and viscoelastic relaxations. Then we compare in detail the two spectra in the terminal region.

The tube theory proposed by Doi and Edwards[15,16] assumes that the stress relaxation under infinitesimal deformation is proportional to the probability that a test chain is still in the original tube in which it was confined at time zero. Thus viscoelastic relaxation in the terminal region reflects orientational relaxation of the end-to-end vector of the chain. In fact the Doi theory[15] predicts that both the viscoelastic and dielectric relaxation spectra should be the same. We test whether this prediction is correct or not. In unentangled bulk polymers, the dynamics of large-scale motions is characterized by the Rouse theory.[12] We also test the Rouse theory by measuring both the shear viscosity and τ_n on the same *cis*-PI samples.

Theory

We briefly review with theories for analyses of viscoelastic and dielectric data. Although many experiments on primary α_a relaxation were made, the shape of loss curves was analyzed with empirical equations such as the Kohlrausch–Williams–Watts[17,18] and Havriliak–Negami[19] equations. An explanation of segmental motions has been made based on the free-volume theory.[1,20] However, there exist no widely accepted molecular theories to describe segmental motions. This is because segmental motions depend strongly on the local chemical structure of the particular polymer, and therefore it is difficult to apply a generalized molecular view to explain the segmental motions.

On the other hand, molecular motions associated with the terminal region are closely related to the autocorrelation function of the end-to-end vector $\mathbf{r}$

$$\phi = \langle \mathbf{r}(0)\cdot\mathbf{r}(t)\rangle / \langle r^2\rangle \qquad (1)$$

where t is time, and $\langle r^2\rangle$, the mean-square end-to-end distance. For a type A polymer[4] having the dipole moment

0024-9297/90/2223-3138$02.50/0

proportional to the end-to-end vector $\mathbf{r}$, the complex dielectric constant ϵ^* is given by[11]

$$\epsilon^* - \epsilon_\infty = \Delta\epsilon \int_0^\infty -(d\phi/dt) \exp(-i\omega t)\, dt \quad (2)$$

where ϵ_∞ is the unrelaxed dielectric constant, $\Delta\epsilon$, the relaxation strength, and ω, the angular frequency. We see that τ_n corresponds to the average correlation time of the autocorrelation function.

For viscoelastic relaxation, on the other hand, the complex viscosity, η^*, is generally given by[21]

$$\eta^* - \eta_\infty = (1/Vk_BT) \int_0^\infty \langle \mathbf{J}(0)\cdot\mathbf{J}(t)\rangle \exp(-i\omega t)\, dt \quad (3)$$

where $\mathbf{J}$ is the momentum flux, and V, the volume. To use eq 3, we need to employ a molecular model and express $\mathbf{J}$ based on the particular model. As discussed later, Doi[15] expressed the correlation function of $\mathbf{J}$ in terms of the tube model.

For unentangled polymers, the autocorrelation function, ϕ, of the end-to-end vector is expressed by the Rouse–Zimm theory.[12,13] Particularly for undiluted polymers hydrodynamic interactions are shielded, and hence the free-draining Rouse model[12] is applicable

$$\phi = (8/\pi^2) \sum (1/p^2) \exp(-t/\tau_p) \quad (4)$$

$$\tau_p = \tau_1/p^2 \qquad p = \text{odd} \quad (5)$$

where p is the number of the normal modes, and only the odd-numbered modes are active for dielectric normal-mode processes. According to the free-draining model, τ_1 is written as

$$\tau_1 = \zeta N\langle r^2\rangle/(3\pi^2 k_BT) \quad (6)$$

where ζ is the monomeric friction coefficient, N, the number of beads, and k_BT, the thermal energy. On the other hand, Zimm[13] indicated that the longest viscoelastic relaxation time, τ_{V1}, is half of the longest dielectric relaxation time, τ_{D1}, given by eq 6:

$$\tau_{D1} = 2\tau_{V1} \quad (7)$$

Then from eq 4, the dielectric relaxation spectrum, $g(\tau_p)$, for the free-draining model is given by

$$g(\tau_p) = (8\Delta\epsilon/\pi_2)(1/p^2) \quad (8)$$

To viscoelastic relaxations, all the odd- and even-numbered (pth) modes contribute equally.[12] Thus the intensity of the viscoelastic relaxation spectrum, $H(\tau)$, is given by

$$H(\tau_p) = k_BT \qquad \text{for all } p \quad (9)$$

If we regard this discrete spectrum as a continuous spectrum, the dielectric and viscoelastic relaxation spectra have a wedge shape with slope $+^1/_2$ and $-^1/_2$, respectively.

On the other hand, the tube model provides a description of the relaxation time of entangled polymers. According to de Gennes[14] and Doi and Edwards,[15,16] the longest relaxation time is given by the tube disengagement time, τ_d

$$\tau_d = L^2/\pi^2 D \quad (10)$$

where L is the length of the tube, and D, the diffusion coefficient of the chain along the tube. The Doi–Edwards theory[16] assumes that the correlation function $\langle \mathbf{r}(0)\cdot\mathbf{r}(t)\rangle$ is proportional to the probability, ψ, that a chain confined in a tube at time 0 is still remaining in the tube. The time dependence of $\langle \mathbf{r}(0)\cdot\mathbf{r}(t)\rangle$ is given by the same form as the Rouse model (eqs 4 and 5) but replacing τ_1 by τ_d. The theory also predicts that the stress relaxation is also proportional to ψ.[16] Thus the normalized $g(\tau)$ and $H(\tau)$ in the entangled regime are the same and have a wedge shape with slope $+^1/_2$.

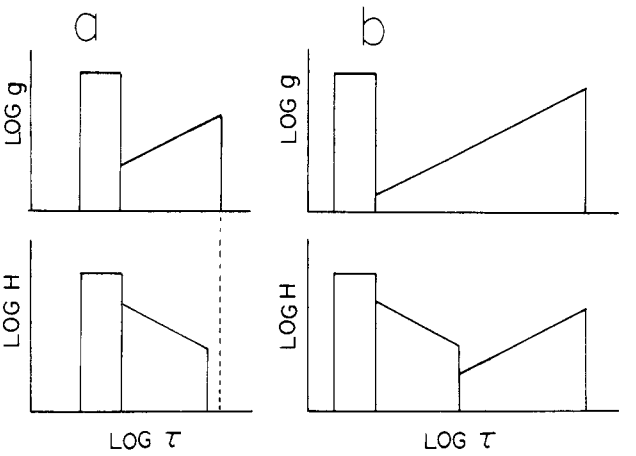

Figure 1. Schematic diagrams of dielectric, $g(\tau)$, and viscoelastic relaxation spectra, $H(\tau)$ of linear type A polymers in the nonentangled regime (a) and those in the entangled regime (b).

Table I
Characteristics of *cis*-PI

code	$10^{-3}M_w$	M_w/M_n	code	$10^{-3}M_w$	M_w/M_n
PI-1.6	1.55	1.11	PI-31	31.2	1.09
PI-2.6	2.64	1.09	PI-32	31.6	1.05
PI-3.5	3.50	1.07	PI-53	52.9	1.08
PI-4.8	4.84	1.07	PI-84	83.8	1.06
PI-5.4	5.37	1.05	PI-140	140	1.05
PI-5.8	5.80	1.08	PI-248	248	1.05
PI-9.5	9.49	1.07	PI-382	382	1.07
PI-21	20.7	1.09	PI-626	626	1.05

Figure 1a shows sketches of $g(\tau)$ and Figure 1b those of $H(\tau)$ for nonentangled (left-hand side) and entangled (right-hand side) type A polymers. Here we assumed that the viscoelastic and dielectric relaxation spectra associated with segmental motions have a narrow box shape. It is noted that generally the intensity of dielectric relaxation spectra for segmental motions depends on the component of the dipole moment perpendicular to the chain backbone. Thus the ratio of the intensities of $g(\tau)$ for the normal- and segmental-mode processes changes from one polymer to another. It is expected that $H(\tau)$ due to segmental motions also depends on the chemical structure of the polymers.

Experimental Section

Samples. Samples of *cis*-PI were prepared by anionic polymerization in heptane with *sec*-butyllithium as the initiator. They were characterized by gel permeation chromatography as described previously.[9,10] The characteristics of the samples are given in Table I.

Methods. Dielectric measurements were carried out mostly with a transformer bridge (General Radio 1615A) in the range of frequency f from 20 Hz to 100 kHz. To cover the frequency range below 20 Hz, we also used a transient current method.[3] Usually measurements of transient current were performed by applying stepwise a direct current (dc) voltage. We found that when dc voltage was applied for a long period, discharging current increased probably due to the electrode polarization caused by impurity ions. We expected that if the polarity of the voltage was reversed at a certain frequency, the artifact due to the electrode polarization could be reduced, since ions migrate only back and forth under the oscillating field. Thus we imposed on the sample a rectangular-shaped voltage of frequency between

0.001 and 10 Hz. The absorption current was measured with a Keithley current amplifier (Model 427). The capacitance of the empty cell was 130 pF, and the amplitude of the rectangular voltage was 10 V. The complex dielectric constant was calculated by Fourier transform of the absorption current. Details of this method will be described elsewhere.[22]

Complex shear modulus G^* was measured with a Rheometrics dynamic spectrometer (Model RDS-II). Shear viscosity, η_0, was measured with a Iwamoto rheometer (Model IR-200).

Calculation of Dielectric Relaxation Spectra. To calculate viscoelastic (or dielectric) relaxation spectra, the second approximation method proposed by Tschoegl[1,23] has been routinely used. However, this method is more applicable to the system with a broad distribution of relaxation times. When a real spectrum has a sharp cutoff or isolated sharp peaks, the Tschoegl method provides a spectrum being smoothed out. Since the ϵ'' curve in the present study is relatively narrow, the Tschoegl method might be insufficient to calculate $g(\tau)$. In this paper, we calculated $g(\tau)$ by a "histogram" method reported recently.[24] The calculation of the spectra was carried out on a microcomputer by a trial and error method so that the difference between the observed ϵ'' and the calculated ϵ'' curve with a trial spectrum became minimum.

Results and Discussion

Viscoelastic and Dielectric Relaxations for Entangled *cis*-PI. Measurement of the shear modulus was carried out on the *cis*-PI samples with a M_w of 8×10^4–6×10^5 in the terminal region. Since the characteristic molecular weight M_e of *cis*-PI is 10 000, these samples are in the entangled regime. The master curves were constructed at 273 K. For the viscoelastic loss curve in the glass–rubber transition region, we used our previous data of the complex Young's moduli E^*(network) of two natural rubber networks.[25] Since the glass–rubber transition is due to local motions, the E^* curve in this region is independent of the molecular weight or the network structure provided that cross-link density is low. Thus we attempted to combine the G'' curves of *cis*-PI and the E'' curve of the networks. For this purpose, G'' was converted into E'' with the relation

$$E = 3G/(1 + G/3B) \tag{11}$$

where B is the compression modulus. Although it is not certain whether this equation also holds for complex moduli E^* and G^*, we may safely assume that $E'' = 3G''$ in the rubbery state because $B \gg G$.

Figure 2b shows the frequency f dependence of the E'' curves thus constructed. Around $\log f = 3$, the $3G''$ curves of *cis*-PIs and the E'' curves of the natural rubber networks agree well. Thus the whole E'' curves shown in Figure 2 can be regarded as the E'' curves of un-cross-linked *cis*-PIs.

The complex dielectric constant ϵ^* of bulk *cis*-PI samples was reported in our previous papers,[9,10] in which we employed the time–temperature superposition principle to obtain the ϵ^* curve over a wide frequency range. In the present study we measured the dielectric loss ϵ'' of PI-140 at 273 K in the frequency range of $-3 < \log f < 1.5$ with an absorption current method.[22] The dielectric measurement was also carried out with the transformer bridge in the range of $1.3 < \log f < 4.7$. Thus we obtained the data of ϵ' and ϵ'' over the range from 0.001 to 5×10^4 Hz without assuming the time–temperature superposition principle. The ϵ'' curve of PI-140 is shown in Figure 2a, where the ϵ'' curve in the range of $\log f > 4.7$ is plotted by shifting the low-temperature data with the shift factor reported previously.[10]

Here it is noted that there are several studies of the time–temperature superposability over wide frequency or time ranges.[1,7] Plazek[26] and Lamb et al.[27,28] indicated that the shift factor for the terminal region and that for the wedge-type spectral region were different. Thus the ϵ'' and E'' curves shown in Figure 2 may be slightly different from the curves measured directly without using the superposition hypothesis. However, we expect that this difference is not serious.

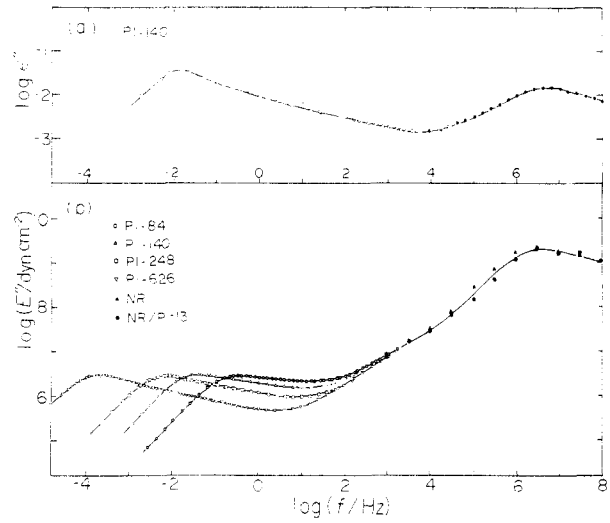

Figure 2. Comparison of the dielectric loss curve of PI-140 (a) and the loss Young's modulus, E'', (b) of PI-84, PI-140, PI-248, and PI-626 at 273 K. The E'' curves above 1000 Hz are those of the natural rubber NR and NR containing PI-13.[25] These curves are obtained by assumption of the time–temperature superposition principle.

We note that the E'' curve of PI-140 is composed of so-called box- and wedge-type regions in $-3 < \log f < 1$ and $1 < \log f$, respectively. The box- and wedge-type regions coincide, respectively, with the frequency ranges where the dielectric normal- and segmental-mode relaxations are observed.

The mechanical relaxation around the maximum of the wedge-type spectrum is known to be associated with glass–rubber transition.[1] Obviously both the viscoelastic and dielectric relaxation in this region are originated from similar local motions. However, we recognize that the loss maximum frequency f_m for the E'' curve is ca. 0.3 decades lower than the ϵ'' curve.

We also note that the slope of the E'' curve in the range of $4.5 < \log f < 6$ is steeper than 0.5 expected from the Rouse theory.[12] This suggests that the E'' curve in this region is reflected by the local segmental motions different from the Rouse-like motions. The behavior that the slope of the G'' or E'' curves in the wedge-type region become steeper than 0.5 around the loss peak was already reported by several authors.[1,29-32] The steepness of the slope depends on the chemical structure of polymers.[1]

Comparison of Dielectric and Viscoelastic Relaxation Spectra over a Wide Frequency Range. The ϵ'' and E'' curves of PI-140 shown in Figure 2 were transformed into the dielectric ($g(\tau)$) and viscoelastic ($H(\tau)$) relaxation spectra, respectively, as shown in Figure 3. We see that the feature of these spectra agree qualitatively with the theoretical expectation for entangled polymers (Figure 1).

In Figure 3 we recognize at least four characteristic times τ_A, τ_B, τ_C, and τ_D as indicated there. As discussed above, τ_A corresponds to the relaxation time for the local segmental motions and τ_D that for the viscous flow process. On the other hand, τ_C corresponds to the transition from the wedge- to box-type spectral regions. Roughly speaking, τ_C is equal to the longest relaxation time of the polymer having the molecular weight between entan-

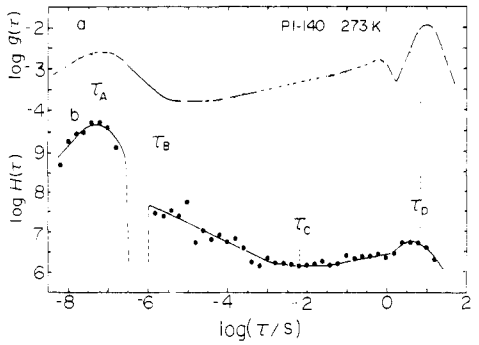

Figure 3. Comparison of the dielectric relaxation spectrum, $g(\tau)$, of PI-140 (a) and the viscoelastic relaxation spectrum, $H(\tau)$, (b) of PI-140 calculated from the data shown in Figure 2. Four characteristic times, τ_A, τ_B, τ_C, and τ_D, are assigned as shown in this figure.

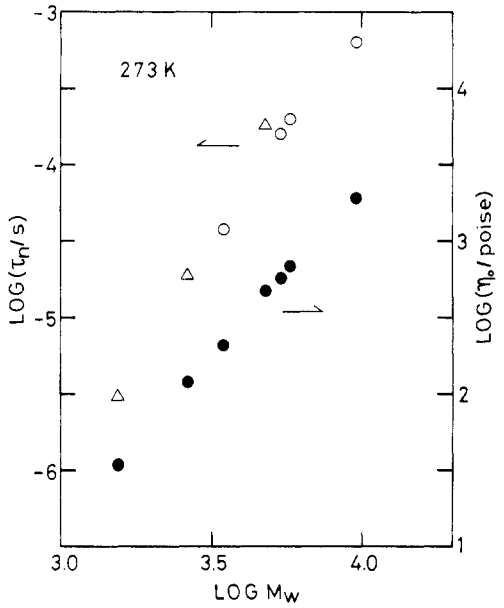

Figure 4. Molecular weight dependence of the relaxation time, τ_n, for the dielectric normal-mode process and zero shear viscosity, η_0, at 273 K for *cis*-PIs with M_w less than the characteristic molecular weight, M_c.

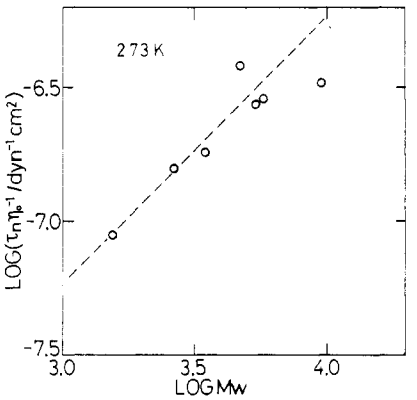

Figure 5. Molecular weight dependence of τ_n/η_0 for *cis*-PI with M_w less than M_c. The dashed line indicates the theoretical value calculated with eq 13.

glement M_e.[1,2] In the range between τ_B and τ_C, the slope of the $H(\tau)$ curve is -0.50 ± 0.05 in agreement with the Rouse theory.[12] We thus consider that τ_B corresponds to the transition between the Rouse-like and the local segmental motions. In other words, τ_B can be assigned to the shortest relaxation time of the Rouse mode.

Usually the number N of beads in the Rouse theory is chosen arbitrary since as far as we are concerned with large scale motions N does not appear in the theoretical quantities. However, to discuss the shortest relaxation time of the Rouse-like motions, we have to specify N. Here we estimated N from τ_B as follows.[12] If *cis*-PI molecules with $M_w = M_e$ (=5000) are modeled by N beads and $N - 1$ springs, the longest relaxation time $\tau_R(M_e)$ is equal to $N^2\tau_B$. From τ_B and the value of $\tau_n(M_e)$ ($=\tau_R$) reported previously,[9,10] the minimum separation of the beads of *cis*-PI is estimated to be 630 in molecular weight or to be 9.3 monomeric units. This indicates that ca. 40 backbone atoms are required for manifestation of rubber elasticity.

In the viscoelastic relaxation spectrum, there is a sharp gap around τ_B, indicating that the spectral regions for the segmental and Rouse-like motions are not continuous. However, since the data points of E'' in the glass–rubber transition region scatter considerably, it is needed to confirm the presence of the gap by a more precise measurement.

Relaxation Time in Terminal Region. In the following sections we compare the dielectric and viscoelastic relaxations in the terminal region. We examine the molecular weight dependence of the dielectric normal-mode relaxation time, τ_n, and the terminal viscoelastic relaxation time, τ_V.

Nonentangled Regime. For low molecular weight *cis*-PIs, τ_V was estimated from the zero shear viscosity, η_0, with the Rouse equation:[12]

$$\tau_V = 6\eta_0 M/(\pi^2 \rho RT) \tag{12}$$

Figure 4 shows the M_w dependence of τ_n and η_0 for the samples with $M_w < M_c$. The slopes of τ_n and η_0 are ca. 3 and 2, respectively, and are higher than the theoretical values of 2.0 for τ_n and 1.0 for η_0.[12] This behavior is well-known for low molecular weight polymers and is attributed to the molecular weight dependence of the friction coefficient, ζ.

The Rouse theory indicates that both τ_n and η_0 are proportional to ζ, and therefore τ_n/η_0 should be independent of ζ:

$$\tau_n/\eta_0 = 12M/(\pi^2 \rho RT) \tag{13}$$

Figure 5 shows a τ_n/η_0 versus M_w plot for the samples with $M_w < M_c$. The dashed line represents eq 13. It is seen that the experimental values agree well with the Rouse theory. Previously we compared τ_n of *cis*-PI in dilute dioxane solutions (θ solution) with the Zimm theory[13] by using the experimental values of the intrinsic viscosity.[34] There we found that the observed τ_n was ca. 0.2 decades longer than the Zimm theory. The present results indicate that in the nonentangled regime eq 6 holds.

In order to discuss the M_w dependence of τ_n and τ_V, it is desirable to compensate the M_w dependence of ζ. Previously we reported that ζ is proportional to the relaxation time for the segmental-mode process, τ_s. If this hypothesis is valid, we expect that $\tau_s\tau_n/\eta_0^2$ is independent of M_w in the range $M_w < M_c$. This is tested in Figure 6. We see that the values of $\tau_s\tau_n/\eta_0^2$ are almost independent of M_w within the error of ± 0.2 decades. This result supports the validity of the hypothesis of $\zeta \propto \tau_s$. However, we see a trend that $\tau_s\tau_n/\eta_0^2$ decreases slightly with increasing M_w. This is attributed to the onset of entanglement in the range of M_w lower than M_c. Since τ_n and η_0 have the same M_w dependence in the entangled region, $\tau_s\tau_n/\eta_0^2$ decreases rapidly with increasing M_w in the range of $M_w > M_c$.

We reported previously that when $M_w > 5000$, τ_s is almost independent of M_w, which is denoted as

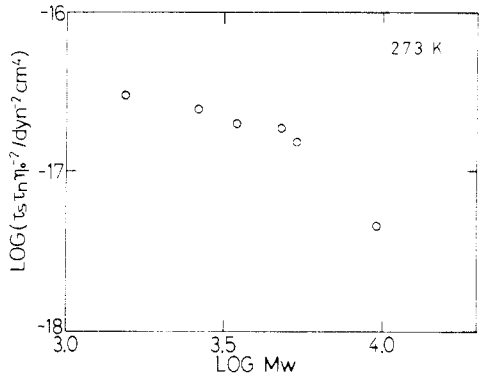

Figure 6. Plot of $\tau_n\tau_s/\eta_0^2$ against M_w.

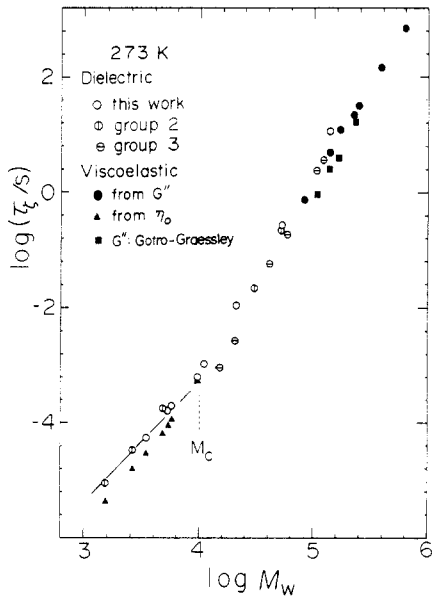

Figure 7. Dielectric and viscoelastic relaxation times at 273 K reduced to the isofriction state.

τ_s(HMW).[9,10] However, for those with $M_w < 5000$, τ_s decreases with decreasing M_w. To compensate the M_w dependence of ζ of low molecular weight *cis*-PIs, the factor of τ_s(HMW)/τ_s was multiplied to τ_n and τ_V for the samples with $M_w < 5000$. The τ_n and τ_V reduced to an isofriction state are denoted as $\tau_{n\zeta}$ and $\tau_{V\zeta}$, respectively, and plotted in Figure 7.

Entangled Region. For the samples with $M_w > M_c$, τ_n and τ_V were determined from the loss maximum frequency, f_m, with the relation $\tau_V = 1/(2\pi f_m)$. In Figure 7, we plotted all available data of τ_n and τ_V for *cis*-PIs with M_w higher than M_c. The data of τ_n are classified into three groups: (1) the data of the present study; (2) the data reported previously[10] for *cis*-PI with $M_w/M_n < 1.08$; and (3) those[9] with $M_w/M_n \simeq 1.2 \pm 0.1$. Though the values τ_n of these groups are approximately the same, we recognize that τ_n for the narrow distribution samples is slightly higher than those for the samples of the group (3).

As is seen in Figure 7, both data of τ_n and τ_V were available only in a narrow M_w region of $5.0 < \log M_w < 5.2$. We see a trend that τ_n is slightly longer than τ_V. However, within an experimental error, we conclude that τ_n agrees with τ_V in the entangled region. This result agrees with the prediction by de Gennes[14] and Doi and Edwards.[16] The viscoelastic relaxations of *cis*-PI having the microstructure similar to the present *cis*-PI samples were reported by Nemoto et al.[35] and by Gotro and Graessley.[36] In Figure 7 we also plotted τ_V determined from f_m of the G'' curves reported by Gotro and Graessley with the key of filled square. The relaxation time τ_V reported by Nemoto et al. was ca. 1 decade longer than τ_n probably due to an error in the shift factor.[9]

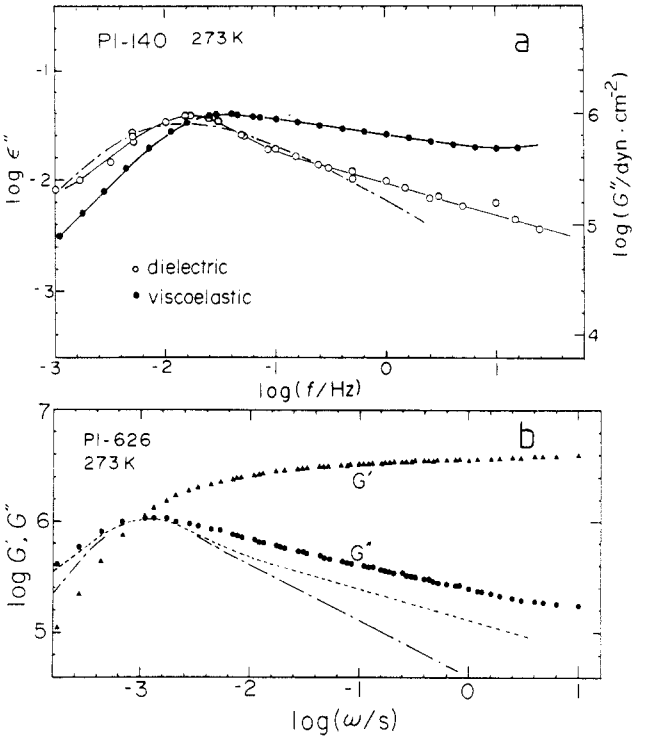

Figure 8. (a) Comparison of the dielectric loss, ϵ'', and the loss shear modulus, G'', of PI-140 at 273 K. Dash-dot line shows the loss curve calculated with the KWW equation with $n = 0.40$ (b) Storage and loss modulus of PI-626. The dashed line indicates the ϵ'' curve of PI-140 shifted so that the maximum of the G'' curve and ϵ'' curve coincide. Dash-dot line indicates the loss curve predicted by Doi and Edwards.

Comparison of Loss Curves for Dielectric and Viscoelastic Relaxations. In this section we compare the distribution of relaxation times for the dielectric and viscoelastic relaxations in the entangled regime. We review briefly the theoretical background. Generally the complex shear viscosity, η^*, is given by eq 3. According to Doi,[15] the correlation function of the momentum flux, $\mathbf{J}(t)$, is expressed as

$$\langle \mathbf{J}(0)\cdot\mathbf{J}(t)\rangle = \frac{(\gamma k_B T)^2 c V}{60b^2}\langle \mathbf{r}(0)\cdot\mathbf{r}(t)\rangle \qquad (14)$$

where $\mathbf{J}$ is the flux averaged over a time domain shorter than the time scale of the end-to-end fluctuation, c, the number of molecules in unit volume, γ, the constant, and b, the average distance between beads. By eliminating $\langle \mathbf{r}(0)\cdot\mathbf{r}(t)\rangle$ from eqs 2, 3, and 14 and using the relationship between η^* and G^*, we obtain

$$1 - \frac{\epsilon^*(\omega)}{\Delta\epsilon} = \frac{\pi^2\tau_d}{12\eta_0}G^*(\omega) \qquad (15)$$

This equation predicts that the log ϵ'' curve and the log G'' curve are superposable. In other words, the viscoelastic relaxation spectrum log $H(\tau)$ and the dielectric relaxation spectrum log $g(\tau)$ should have exactly the same shape.

Turning to the experimental results, we compare the ϵ'' and G'' curves for PI-140 in Figure 8a. As mentioned above, τ_V is slightly shorter than τ_n. We note that the G'' curve is much broader than the ϵ'' curve. This is partly due to the overlapping of the G'' curve due to the wedge-type spectrum that appears in the range between τ_B and τ_C in Figure 3. Therefore M_w of 1.4×10^5 is still too low

to compare the ϵ'' and G'' curves in the terminal region. Since the separation of the terminal and wedge-type regions increases with increasing molecular weight, we compared the ϵ'' curve of PI-140 with the G'' curve of PI-626 in Figure 8b. However, it is seen that the ϵ'' curve plotted with a dashed line is still narrower than the G'' curve. Thus we conclude that eq 15 does not hold at least for *cis*-PI. The dash-dot line represents the theoretical loss curve calculated with eq 8. As pointed out previously[9,10] the ϵ'' curve is broader than the Doi–Edwards and Rouse theories.

So far we discussed our data based on the tube theory. A completely different approach was made by Ngai and his co-workers[37,38] who proposed a coupling theory. This theory predicts that dielectric and mechanical relaxations in the terminal region are expressed by the Fourier transform of the KWW type correlation function[17,18]

$$\phi(t) = \exp[-(t/\tau_K)^{1-n}] \quad (16)$$

where n is the parameter and τ_K the nominal relaxation time. Ngai and Rendell[39] determined n to be 0.40–0.46 for the dielectric normal-mode process of linear and star-shaped polyisoprenes reported by us and by Boese et al.[40] In Figure 8a, the loss curve calculated with the KWW equation with $n = 0.40$ is shown. It is seen that the observed ϵ'' curve agrees roughly with the KWW equation.

Ngai and his co-workers compared the value of n obtained from the dielectric data with n for the viscoelastic relaxation of hydrogenated polybutadiene,[41,42] which exhibited $n = 0.41$. These analyses by Ngai and his co-workers[38] suggest that the shapes of the dielectric and viscoelastic loss curves are the same. This contradicts the conclusion of the present study. It is emphasized that in the present study, the comparison was made for the same sample, and hence our conclusion may be more reliable.

Ngai and his co-workers also calculated the molecular weight dependence of the longest relaxation time in an entangled regime and predicted that $\tau \propto M^{2/(1-n)}$. With $n = 0.44$, the exponent of M becomes 3.6, in excellent agreement with the present results shown in Figure 7.

Comparison of Dielectric and Mechanical Relaxation Spectra. To compare the difference between the dielectric and viscoelastic relaxation behavior in more detail, we converted the ϵ'' and G'' curves of PI-53 and PI-140 and the G'' curve of PI-626 into the relaxation spectra. The results are shown in Figure 9.

Previously we calculated $g(\tau)$ of narrow distribution samples of *cis*-PIs with M_w less than 32 000.[24] The general feature of $g(\tau)$ is that there is a main peak in the longest relaxation time region and that there exists a sharp cutoff of the spectra in the region longer than the relaxation time for the main peak. In the time region of 1 decade shorter than the main peak, we recognize a weak subpeak. The intensity of this subpeak increased with increasing molecular weight.

A similar trend is seen in $g(\tau)$ of PI-53 and PI-140. We see that the resolution of the main and secondary peaks becomes more clear than that for the low molecular weight *cis*-PIs.[24] In the shorter time region, a broad and continuous spectrum is seen. The slope of the spectrum in this region is $^1/_3$ to $^1/_4$ and is lower than the theoretical slope of $^1/_2$ (see Figure 1) as reported previously.[24]

On the other hand, $H(\tau)$ of PI-626 also exhibits a main peak at the longest relaxation time region. However, no side peak is seen in $H(\tau)$. This is the most clear difference between the viscoelastic and dielectric spectra. This result does not agree with the tube theory in two aspects. First, if the proportionality between $\langle \mathbf{J}(0)\cdot\mathbf{J}(t)\rangle$ and $\langle \mathbf{r}(0)\cdot\mathbf{r}(t)\rangle$ given by eq 14 holds, $g(\tau)$ and $H(\tau)$ have the same distribution. Figure 9 shows eq 14 does not hold. Second, both $g(\tau)$ or $H(\tau)$ do not coincide with the theoretical spectrum given by eqs 4 and 5.

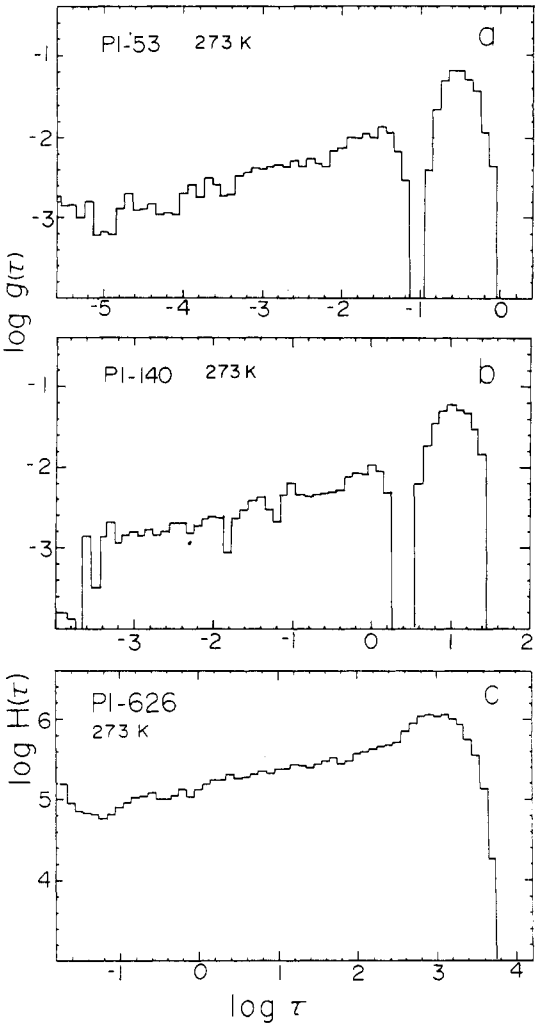

Figure 9. Comparison of the dielectric relaxation spectra of PI-53 and PI-140 and the viscoelastic relaxation spectrum of PI-626 in the terminal region.

Conclusions

1. Dielectric relaxation times for the normal- and segmental-mode relaxations coincide approximately with the viscoelastic relaxation times for the rubber–liquid and glass–leather transitions, respectively.
2. In the intermediate time region, the slope of the viscoelastic relaxation spectrum is $-^1/_2$, but that of dielectric relaxation spectrum is $+^1/_3$ to $+^1/_4$.
3. In the terminal region the distribution of relaxation times for dielectric relaxation is narrower than that for viscoelastic relaxation.
4. The dielectric relaxation spectrum has a side peak, but the viscoelastic relaxation spectrum does not.

Acknowledgment. We thank Rheometrics Far East Co. for kindly allowing us to use the rheometer (RDS-II). This work was supported in part by the Grant-in-Aid for Scientific Research by the Ministry of Education, Science and Culture (C6055062 and A63303010). Support from the Institute of Polymer Research, Osaka

University, is also gratefully acknowledged.

References and Notes

(1) Ferry, J. D. *Viscoelastic Properties of Polymers*; Wiley: New York, 1961.
(2) Graessley, W. W. *Adv. Polym. Sci.* **1974**, *16*, 1.
(3) McCrum, N. G.; Read, B. E.; Williams, G. *Unelastic and Dielectric Effects in Polymeric Solids*; Wiley: New York, 1967.
(4) Stockmayer, W. H. *Pure Appl. Chem.* **1967**, *15*, 539.
(5) North, A. M.; Phillips, P. J. *Trans. Faraday Soc.* **1967**, *63*, 1537.
(6) Ngai, K. L.; Mashimo, S.; Fytas, G. *Macromolecules* **1988**, *21*, 3030.
(7) Fytas, G.; Ngai, K. L. *Macromolecules* **1988**, *21*, 804.
(8) Adachi, K.; Kotaka, T. *Macromolecules* **1984**, *17*, 120.
(9) Adachi, K.; Kotaka, T. *Macromolecules* **1985**, *18*, 466.
(10) Imanishi, Y.; Adachi, K.; Kotaka, T. *J. Chem. Phys.* **1988**, *89*, 7585.
(11) Adachi, K.; Kotaka, T. *Macromolecules* **1988**, *21*, 157.
(12) Rouse, P. E. *J. Chem. Phys.* **1953**, *21*, 1272.
(13) Zimm, B. H. *J. Chem. Phys.* **1956**, *24*, 269.
(14) de Gennes, P.-G. *J. Chem. Phys.* **1971**, *55*, 572.
(15) Doi, M. *Chem. Phys. Lett.* **1974**, *26*, 269.
(16) Doi, M.; Edwards, S. F. *J. Chem. Soc., Faraday Trans. 2* **1978**, *74*, 1789, 1802, 1818.
(17) Williams, G.; Watts, D. C. *Trans. Faraday Soc.* **1971**, *66*, 80.
(18) Kohlrausch, R. *Prog. Ann. Phys.* **1847**, *12*, 393.
(19) Havriliak, S.; Negami, S. *J. Polym. Sci. Part C* **1966**, *No. 14*, 99.
(20) Williams, M. L.; Landel, R. F.; Ferry, J. D. *J. Am. Chem. Soc.* **1955**, *77*, 3701.
(21) Zwanzig, R. *Annu. Rev. Phys. Chem.* **1965**, *16*, 67.
(22) Adachi, K.; Fukui, F.; Kotaka, T., to be submitted for publication in *Polym. J.*
(23) Tschoegl, N. W. *Rheol. Acta* **1971**, *10*, 582.
(24) Imanishi, Y.; Adachi, K.; Kotaka, T. *J. Chem. Phys.* **1988**, *89*, 7593.
(25) Poh, B. T.; Adachi, K.; Kotaka, T. *Macromolecules* **1987**, *20*, 2563, 2569, 2574.
(26) Plazek, D. J. *J. Phys. Chem.* **1965**, *69*, 3480.
(27) Gray, R.; Harrison, G.; Lamb, J. *Proc. R. Soc. London* **1977**, *356*, 77.
(28) Cochrane, J.; Harrison, G.; Lamb, J. *Polymer* **1980**, *21*, 837.
(29) Williams, M. L.; Ferry, J. D. *J. Colloid Sci.* **1954**, *9*, 479.
(30) Yin, T. P.; Ferry, J. D. *J. Colloid Sci.* **1961**, *16*, 166.
(31) Fujino, K.; Senshu, K.; Kawai, H. *J. Colloid Sci.* **1961**, *16*, 262.
(32) Kurath, S. F.; Passaglia, E.; Pariser, R. *J. Appl. Phys.* **1957**, *28*, 499.
(33) Aklonis, J. J.; Tobolsly, A. V. *J. Appl. Phys.* **1965**, *36*, 3483.
(34) Adachi, K.; Kotaka, T. *Macromolecules* **1987**, *20*, 2018.
(35) Nemoto, N.; Odani, H.; Kurata, M. *Macromolecules* **1972**, *5*, 531.
(36) Gotro, J. T.; Graessley, W. W. *Macromolecules* **1984**, *17*, 2767.
(37) Ngai, K. L. *Comments Solid State Phys.* **1979**, *9*, 127.
(38) Ngai, K. L.; Rendell, R. W.; Rajagopal, A. K.; Teitler, S. *Ann. N.Y. Acad. Sci.* **1986**, *484*, 150.
(39) Nagi, K. L.; Rendell, R. W. *Polym. Prepr.* **1989**, *30*, 89.
(40) Boese, D.; Kremer, F.; Fetters, L. J. *Makromol. Chem., Rapid Commun.* **1988**, *9*, 367.
(41) Ngai, K. L.; Plazek, D. J. *J. Polym. Sci., Polym. Phys. Ed.* **1985**, *23*, 2159.
(42) Mckenna, G. B.; Ngai, K. L.; Plazek, D. J. *Polymer* **1985**, *26*, 1651.

Viscoelastic Properties of Simple Flexible and Semirigid Models from Brownian Dynamics Simulation

F. Guillermo Díaz and José García de la Torre*

Departamento de Química Física, Universidad de Murcia, Espinardo, 30100 Murcia, Spain

Juan J. Freire

Departamento de Química Física, Facultad de Química, Universidad Complutense, 28040 Madrid, Spain

Received June 22, 1989; Revised Manuscript Received November 27, 1989

ABSTRACT: A Brownian dynamics simulation procedure to obtain the frequency dependence of the complex solution viscosity of macromolecular models is presented. From simulated trajectories, data for the time-autocorrelation function of a component of the momentum-flux tensor are obtained. After the simulated data are fitted to a mono- or multiexponential function, the frequency-dependent viscosity is obtained according to the Green–Kubo formula. The results of this procedure are checked against theoretical prediction for four different models: the quasirigid dumbbell, the Gaussian dumbbell, the semiflexible trumbbell, and Gaussian chains.

Introduction

The complex interplay existing between shape or flexibility, hydrodynamic interactions, and, eventually, solvent flow makes it practically impossible to find analytical solutions for many problems in polymer hydrodynamics.[1,2] A useful alternative, or complement, to analytical theory is the computer simulation of the Brownian dynamics of the polymer. In the field of flexible macromolecules, Brownian dynamics simulation has been used to study fluctuating hydrodynamic interactions,[3-5] internal modes,[6] elongation in flows,[7-9] and shear-dependent rheological properties.[9,10] For semiflexible macromolecules, Brownian dynamics has been used in the study of wormlike chains[11,12] and segmentally flexible macromolecules.[13,14]

The simulation of the intrinsic viscosity and its frequency dependence has not received enough attention. The zero-shear, zero-frequency viscosity can be obtained from shear rate dependent viscosities obtained by simulation.[9,10] This procedure is rather influenced by the

* To whom correspondence should be addressed.

0024-9297/90/2223-3144$02.50/0